J Low Temp Phys (2012) 167:280–285
DOI 10.1007/s10909-012-0539-1

High Energy Resolution Cryogenic Alpha Spectrometers Using Magnetic Calorimeters

W.S. Yoon · Y.S. Jang · G.B. Kim · K.J. Kim · M.S. Kim · J.S. Lee · K.B. Lee · M.K. Lee · S.J. Lee · H.J. Lee · Y.N. Yuryev · Y.H. Kim

Received: 31 July 2011 / Accepted: 10 January 2012 / Published online: 27 January 2012

Abstract We report the recent progress on high resolution alpha spectrometers that use metallic magnetic calorimeters. The detector is composed of a meander-type magnetic calorimeter and a gold-foil absorber. The thermal connection between the magnetic sensor and the absorber consists of annealed gold wires. The signal rise time is found to be as expected, with the electronic thermal conductance of gold wires. The energy resolution of a 3.2 keV FWHM is obtained for 5.5 MeV alpha particles with possibilities for further improvements.

Keywords Cryogenic detectors · Metallic magnetic calorimeter · Alpha spectroscopy · High energy resolution

1 Introduction

A metallic magnetic calorimeter (MMC) is one type of low-temperature detectors that have demonstrated high energy resolution. A paramagnetic material (gold doped with erbium, Au:Er) is used as a temperature sensor in an MMC [1]. In many applications in radiation detection and measurement, MMCs have been used as high-energy resolution detectors. They have played significant roles in X-ray spectrometers [2, 3], neutrino mass [4] and beta decay experiments [5] in the keV energy range. An energy resolution of 2.7 eV FWHM was achieved for 6 keV X-rays [3]. This detection method has recently been adopted in alpha spectrometry [6] and in double beta decay experiments [7].

W.S. Yoon · Y.S. Jang · G.B. Kim · K.J. Kim · M.S. Kim · J.S. Lee · K.B. Lee · M.K. Lee · S.J. Lee · H.J. Lee · Y.N. Yuryev · Y.H. Kim (✉)
Korea Research Institute of Standards and Science (KRISS), Daejeon 305-340, Korea
e-mail: yhkim@kriss.re.kr

W.S. Yoon · H.J. Lee · Y.H. Kim
University of Science and Technology, Daejeon 305-333, Korea

The alpha spectrometers with cryogenic detector whose energy resolution exceeds the theoretical limit of the conventional silicon based detector by the number statistics of electron-hole pairs (8 keV FWHM for 3–6 MeV [8]) which has been important analytic tools for nuclear forensic and environmental monitoring [9]. The detectors based on transition edge sensor (TES) technology have shown a resolution about 1 keV for 5.3 MeV alphas from a ^{210}Po source [10]. For plutonium isotopes, a 2.6 keV FWHM was achieved [9]. An alpha spectrometer using a MMC showed an energy resolution of 2.8 keV FWHM for 5.5 MeV alphas from an ^{241}Am source [6]. A large meander-type MMC [3] with a 6.3 mm^2 area gold absorber is introduced for the calorimetric measurement of alpha particles.

We report the recent progress on high resolution alpha spectrometers based on the MMC technology. Following the work in the previous report [6], this experimental work uses the similar setup of the meander-shaped magnetic sensor and the gold absorber. However, the thermal connection between the sensor and the absorber is made with annealed gold wires while it was a direct press contact with a semi-permanent glue (Stycast1266) in the previous work. In the present work the absorber is located next to the meander chip. The thermal connection method using the gold wires is motivated by a few reasons. The thermal conductance via electronic heat conduction can be controllable to avoid an unexpected long rise-time of the signals found in the previous experiment. Easy replacement of the gold absorber is another advantage, instead of the complete sensor-absorber package. For applications in a Q spectrometer using a 4π absorber [11], this thermal connection method is favorable because the 4π absorber is subject to changes in the next experiment with a new sample.

2 Detector Structure

A simplified detection scheme of the alpha spectrometer is shown in Fig. 1. The details of the SQUID and the meander-shaped coil setup were explained in the previous report [6]. The main difference in the current experiment is the location of the gold absorber which was glued onto a separate G10 epoxy substrate. Five gold wires with a diameter of 25 μm and a length of 1.2 mm provided the thermal connection between the magnetic sensor and the absorber. They were bonded onto the side of the absorber and onto five gold stems covering the sensor surface. The 25 μm gold wires, which were annealed, had a resistivity of 1.7 mΩ/mm at 4.2 K.

A commercial thin-layer ^{238}Pu source is used to test the detector performance in the present experiment. In the apparatus, a silver collimator is introduced to prevent direct absorption in the magnetic sensor or in the gold wires. When an alpha particle hits the gold absorber, the absorber is thermalized in a short time. Next, the heat flows into the magnetic sensor through the gold wires. The thermal connection between the sensor and the sample holder that serves as the heat bath is made through the sapphire substrate. It is much weaker than the thermal connection between the sensor and the absorber in order to have a relatively slow decay time compared to the signal rise time. The thermal leak between the absorber and holder is set to be weak by using a small amount of glue (GE varnish) to limit the direct heat flow to the bath. This method guarantees that most of the heat generated by an energy absorption of an

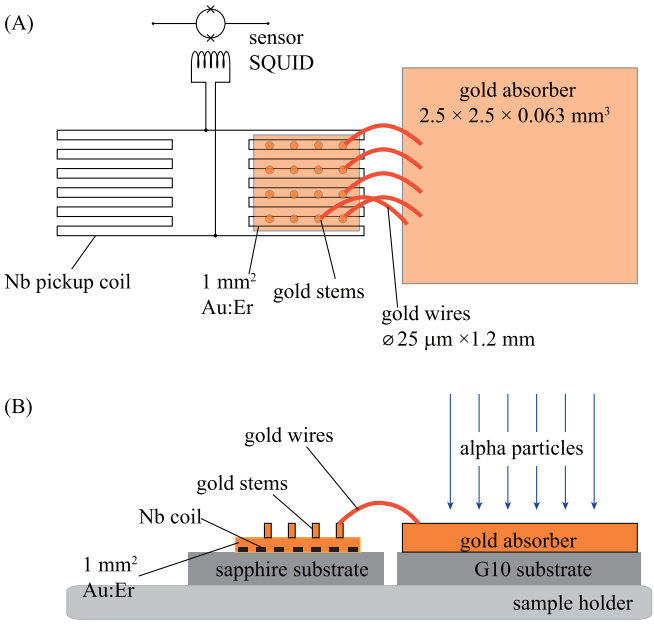

Fig. 1 (Color online) A schematic diagram of the alpha spectrometer using a meander-type MMC. (**A**) The simplified detector design. The simplified circuit shows a two-sided meander coil and an input coil of sensor SQUID. They are connected in a gradiometric configuration along the two sides of the meander coil. Au:Er sensor of 1 mm^2 is sputtered on one side of the meander pickup coil. Sixteen stems are made for thermal connection to a absorber. (**B**) A cross-sectional view of the alpha spectrometer

alpha particle will flow via the gold wires, the sensor, the sapphire substrate, and eventually into the sample holder.

3 Results and Discussion

The energy spectrum measured at 40 mK with the current setup is shown in Fig. 2. A field current of 140 mA was applied to the meander coil in a persistent mode at 40 mK. Two clear peaks appeared at the two major alpha lines of ^{238}Pu. The solid curve indicates the best fit to the measured spectrum.The tailed Gaussian functions that account for the straggling effect are used for the fitting [10]. The corresponding FWHM is 3.2 keV. The inset shows the full energy spectrum of the ^{238}Pu spectrum, which was taken with a low trigger level. It indicates that the spectrometer covers a wide dynamic range of incident energy, and no peaks appear other than the ^{238}Pu lines.

The lattice damage in the absorber caused by the incident alpha particle may result in the intrinsic energy resolution of all of the alpha spectrometers in a solid state. The statistical fluctuations of the Frankel pairs created in a tin absorber are likely responsible for 1 keV broadening of the ^{210}Po spectrum [10]. The present resolution of this detector does not confirm the lattice damage effect in a gold absorber. The random baseline noise of the measurement setup yields a 1.93 keV FWHM alpha

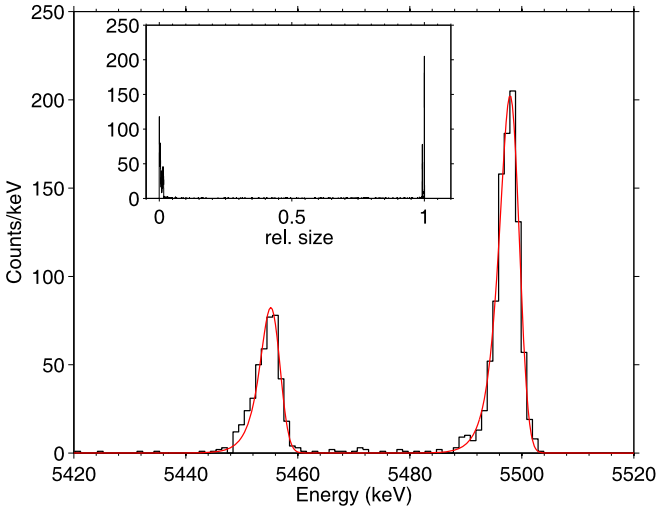

Fig. 2 (Color online) The alpha spectrum of a ^{238}Pu source. The curve is the best fit of the histogram with a Gaussian width of 3.2 keV FWHM and a straggling parameter [10] of 1.6 keV. The *inset* shows a full pulse height spectrum with the pulse size relative to that of the major alpha line

energy equivalent, which is approximately two times larger than the lattice damage effect. The signal-to-noise ratio can be improved when an optimally designed sensor SQUID for the meander is used. The sensor SQUIDs used in the experiments have a self-inductance of about 40 nH, which is slightly larger than the meander inductance. The self-inductance of a sensor SQUID should be about the half of the meander inductance in an optimal case.

Moreover, the measured resolution of the alpha lines is affected by the temperature regulation instability. The temperature and dc level of signal changed over a long time scale with a magnitude of approximately 40 μK. The signal size also varied as the temperature changed because of the temperature dependence of the heat capacities and the magnetization. The spectrum in Fig. 2 is obtained with an optimal filtering method that accounts for an non-stationary behavior [12] of the temperature instability. Further improvements in the signal-to-noise-ratio and in temperature regulation are needed for better resolution.

The signal rise time is compared for the two experiments in which the thermal connections between the absorber and the sensor are made differently. In the previous experiment, a gold foil absorber was firmly pressed onto the stems with a small amount of Stycast1266 epoxy between the meander and the absorber. This direct press contact provided an electrical contact of less than 1 Ω. However, the electronic thermal conductance of the direct contact connection is difficult to estimate because the low-temperature resistance is unknown. In contrast, the thermal connection formed by the gold wires that was used in this experiment can be estimated accurately. The effective resistance of the five gold wires is 408 μΩ at low temperatures, which was calculated from the measured resistance. The electronic thermal conductance, G, can be found as $G = L_0/R_{\text{wire}} \cdot T$ according to the Wiedemann-Franz law where L_0 is the Lorenz number (2.45×10^{-8} W Ω/K^2), R_{wire} is the effective resistance of the gold wires,

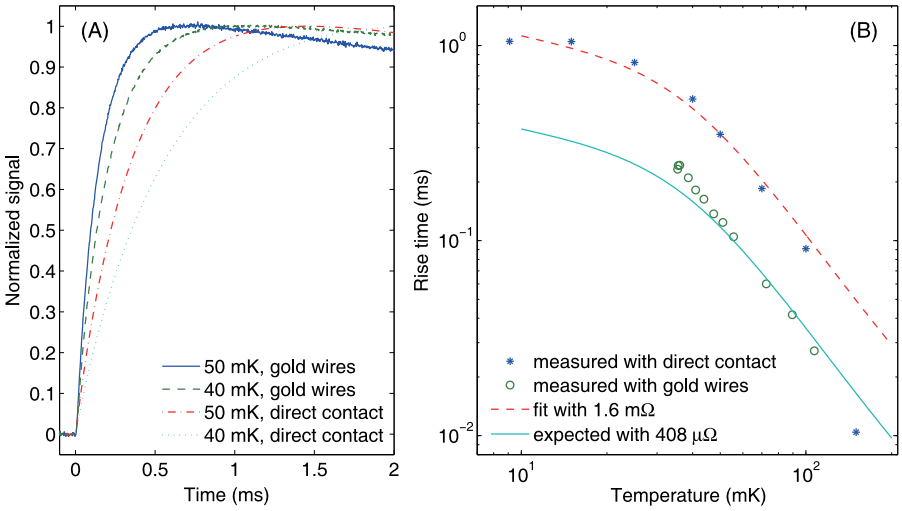

Fig. 3 (Color online) (**A**) The rise of the normalized signals at 40 and 50 mK in the two experiments with either direct thermal contact or five gold wires to establish the thermal connection between the absorber and sensor. (**B**) The rise time of the pulses in the two experiments. The *solid line* is the expected rise time for the electronic thermal conductance calculated from Wiedemann-Franz law with 408 μΩ. The *dashed line* is a guide for the eye with a 1.6 mΩ contact between the absorber and the sensor

and T is the temperature. With a known G and known heat capacities of the gold absorber and the magnetic sensor [1], the time constant that is needed to reach thermal equilibrium between the two thermal systems can be readily estimated.

Figure 3 shows the rise time of the measured alpha pulses with a 140 mA field current. The experiment with gold wire connection shows a faster time constant at all of the temperatures. Here, the rise time constant is defined as the time it takes for the pulse to reach 63.2% $(1-1/e)$ of the full pulse height from the beginning of the pulse. It is convenient to compare this definition to the C_{eff}/G time constant, where C_{eff} is the effective heat capacity of the two thermal systems of the magnetic sensor and the absorber (i.e. $1/C_{\mathrm{eff}} = 1/C_m + 1/C_a$). Here, C_m is the heat capacity of the magnetic sensor. It accounts for the magnetic heat capacity in the magnetic field produced by the meander coil, the electronic heat capacity of gold volume in the sensor, and the heat capacity associated with the nuclear quadrupole moment of the gold nuclei in an electric field gradient in the presence of erbium in the gold lattice. C_a is the electronic heat capacity of gold absorber, which is proportional to the temperature.

At 100 mK, C_a is approximately 10 times larger than C_m, such that $C_{\mathrm{eff}} \approx C_m$. C_m and C_a are equal near 30 mK with a 140 mA field current. Below 30 mK, C_{eff} is close to C_a. In the temperature region C_{eff}/G becomes less sensitive to the temperature because both of the variables are proportional to the temperature. As shown in Fig. 3, the measured values for the thermal connection with the gold wires agree reasonably well with the expected values for the thermal conductance calculated from the Wiedemann-Franz law. The temperature dependence of the measured values shows the tendency that is expected from the heat capacities and thermal conductance. For the experiment with direct thermal contact, the measured values seem to follow well,

with an electronic thermal conductance for a 1.6 mΩ contact resistance. The previous measurement was made in a dilution refrigerator with a base temperature below 10 mK, while this experiment was conducted in an ADR.

4 Conclusions

A new thermal connection method using gold wires has been tested to control the thermal conductance between the absorber and the sensor. It resulted in a faster rise time compared with previous experiment, and the measured values were found as expected. The energy resolution obtained with the alpha spectrometer is not the best energy resolution that MMCs can achieve. However, it can provide adequate resolution for the identification and measurement of most of the radionuclides of interest. The alpha spectrometer using a better combination of SQUID/menader pick-up coil and operating with improved temperature stability will exhibit an extreme sensitivity.

Acknowledgements We thank the Low Temperature Detector group at KIP for supplying the magnetic sensors. This work was supported by the National Research Foundation of Korea Grant funded by the Korean Government (NRF-2011-220-C00006) and Radiation Technology Development Program funded by MEST.

References

1. A. Fleischmann, C. Enss, G.M. Seidel, Top. Appl. Phys. **99**, 151 (2005)
2. L. Fleischmann, M. Linck, A. Burck, C. Domesle, S. Kempf, A. Pabinger, C. Pies et al., IEEE Trans. Appl. Supercond. **19**, 63 (2009)
3. A. Fleischmann, L. Gastaldo, S. Kempf, A. Kirsch, A. Pabinger, C. Pies, J.-P. Porst et al., AIP Conf. Proc. **1185**, 571 (2009)
4. L. Gastaldo, J.P. Porst, F. Von Seggern, A. Kirsch, P. Ranitzsch, A. Fleischmann, C. Enss, G.M. Seidel, AIP Conf. Proc. **1185**, 607 (2009)
5. M. Loidl, M. Rodrigues, B. Censier, S. Kowalski, X. Mougeot, P. Cassette, T. Branger, D. Lacour, Appl. Radiat. Isot. **68**, 1454 (2010)
6. P.C. Ranitzsch, S. Kempf, A. Pabinger, C. Pies, J.-P. Porst, S. Schäfer, A. Fleischmann, L. Gastaldo, C. Enss, Y.S. Jang, I.H. Kim, M.S. Kim, Y.H. Kim et al., Nucl. Instrum. Methods Phys. Res., Sect. A, Accel. Spectrom. Detect. Assoc. Equip. **652**, 299 (2011)
7. S.J. Lee, J.H. Choi, F.A. Danevich, Y.S. Jang et al., Astropart. Phys. **34**, 732 (2011)
8. E. Steinbauer, P. Bauer, M. Geretschläger, G. Bortels, J.P. Biersack, P. Burger, Nucl. Instrum. Methods Phys. Res., Sect. B, Beam Interact. Mater. Atoms **85**, 642 (1994)
9. M.P. Croce, M.K. Bacrania, E.M. Bond, D.E. Dry, A.L. Klingensmith et al., IEEE Trans. Appl. Supercond. **21**, 207 (2011)
10. R.D. Horansky, G.M. Stiehl, J.A. Beall, K.D. Irwin, A.A. Plionis, M.W. Rabin, J.N. Ullom, J. Appl. Phys. **107**, 044512 (2010)
11. S.J. Lee, M.K. Lee, Y.S. Jang, I.H. Kim, S.K. Kim, J.S. Lee, K.B. Lee, Y.H. Lee, Y.H. Kim, J. Phys. G, Nucl. Part. Phys. **37**, 055103 (2010)
12. Y.N. Yuryev, Y.S. Jang, S.K. Kim, K.B. Lee, M.K. Lee, S.J. Lee, W.S. Yoon, Y.H. Kim, Nucl. Instrum. Methods Phys. Res., Sect. A, Accel. Spectrom. Detect. Assoc. Equip. **635**, 82 (2011)